Isgur-Wise function and V_{cb} from Bethe-Salpeter equations

A. Abd El-Hady, K. S. Gupta, A. J. Sommerer, J. Spence, and J. P. Vary
Department of Physics and Astronomy, Iowa State University, Ames, Iowa 50011
(Received 14 December 1994)

We calculate the Isgur-Wise function from the solutions of the Bethe-Salpeter equations. The shape of the Isgur-Wise function thus calculated is a prediction of the Bethe-Salpeter equations and does not depend on undetermined parameters. We develop a best fit to the numerically computed Isgur-Wise function in the form $\xi(\omega) = \eta[1 - \frac{\rho^2}{\eta}(\omega - 1) + a(\omega - 1)^{3/2}]$, where $\rho^2 = 1.279$, $a = 0.91$, $\eta = 0.9942$, and ω is the recoil velocity. The Isgur-Wise function is then used to obtain V_{cb} from the recent experimental data of $\bar{B} \to D^* \ell \bar{\nu}$ decay. Our best estimate of V_{cb} is $(34.7 \pm 2.5) \times 10^{-3}$, which is comparable to some of the latest estimates in the literature.

PACS number(s): 12.15.Hh, 11.10.St, 12.39.Hg, 13.20.He

I. INTRODUCTION

Heavy quark effective theory (HQET) [1–4] has opened a new window for the determination of the Cabibbo-Kobayashi-Maskawa (CKM) matrix elements [4–6]. In particular, determination of V_{cb} using theoretical predictions of HQET and experimental measurement of the differential decay rate of the exclusive semileptonic decay $\bar{B} \to D^* \ell \bar{\nu}$ has received a great deal of attention. With the recent high-precision data available from several experimental groups [7–9], it is now possible to determine the value of V_{cb} with reasonable accuracy.

In order to extract V_{cb} from the experimental data, one needs to calculate hadronic form factors which include nonperturbative effects. HQET has vastly simplified these calculations and only one universal function, called the Isgur-Wise (IW) function [1, 4, 10], has been shown to play a central role in many calculations involving decay of heavy mesons. The calculation of the IW function, however, is model dependent and several different parametrizations for it have been used in the literature [4, 6]. After a particular parametrization is chosen, one typically fits the experimental data to extract the unknown parameter(s) in the IW function as well as V_{cb} from the experimental data.

In this paper we use a covariant reduction of the Bethe-Salpeter equation (BSE) [11] to calculate the IW function [12]. The BSE was solved numerically and the parameters appearing in it (namely, the quark masses, string tension, and the running coupling strength for one-gluon exchange) were determined by fitting the calculated spectrum to the observed masses of more than 40 mesons [13, 14]. The resulting meson mass spectrum agrees very well with the experimental data. Once the parameters are thus fixed, the meson wave functions from the BSE can be used to predict physical observables. In particular, the IW function may then be evaluated from the wave functions of the BSE and would represent a *prediction* independent of any undetermined parameters. Knowing the shape of the IW function we can then extract V_{cb} from the experimental data.

This paper is organized as follows: In Sec. II we recall the main ingredients for the calculation coming from HQET. Section III describes the salient features of the BSE and describes the meson wave functions of interest. In Sec. IV we calculate the IW function and extract V_{cb} from the experimental data. We conclude the paper in Sec. V with a brief outline of future work.

II. HEAVY MESON DECAY FORM FACTORS

The hadronic matrix elements for the decay $\bar{B} \to D^* \ell \bar{\nu}$ take a simple form when described in the context of HQET. Such decays are mediated by heavy quark currents $V_\mu = \bar{c}\gamma_\mu b$ and $A_\mu = \bar{c}\gamma_\mu\gamma_5 b$ and the corresponding matrix elements are in general described in terms of four form factors [1, 10] denoted by ξ_i, $i = 1, 2, 3, 4$:

$$\begin{aligned}\langle D^*(v',\epsilon)|V^\mu|\bar{B}(v)\rangle &= i\sqrt{m_B m_{D^*}}\,\xi_1(\omega)\epsilon^{\mu\nu\alpha\beta}\epsilon^*_\nu v'_\alpha v_\beta\,,\\ \langle D^*(v',\epsilon)|A^\mu|\bar{B}(v)\rangle &= \sqrt{m_B m_{D^*}}\,\xi_2(\omega)\,(\omega+1)\,\epsilon^{*\mu}\\ &\quad -[\xi_3(\omega)\,v^\mu + \xi_4(\omega)v'^\mu]\epsilon^*\cdot v,\end{aligned} \tag{2.1}$$

where $\omega = v \cdot v'$, v and v' being the velocities of $\bar{B}$ and D^* mesons, respectively.

In the limit where masses of the heavy quarks tend to infinity, the form factors ξ_i satisfy the conditions

$$\xi_1 = \xi_2 = \xi_4 \equiv \xi(v \cdot v'), \qquad \xi_3 = 0, \tag{2.2}$$

where $\xi(v \cdot v')$ is a single universal function, called the IW function [1, 4]. In the limit of infinitely heavy quark masses the IW function is normalized to unity at zero recoil; i.e., $\xi(1) = 1$.

The IW function can be related to the overlap integral of normalized meson wave functions in the infinite momentum frame. If $\psi_{l\bar{B}}$ and ψ_{lD^*} denote the wave functions of the light degrees of freedom in $\bar{B}$ and D^* mesons, respectively, then the IW function can be written as

$$\xi(\omega) = \left(\frac{2}{\omega+1}\right)^{1/2} \int \psi^*_{lD^*}(v')\psi_{l\bar{B}}(v)d^3x. \tag{2.3}$$

In the heavy quark limit close to $\omega = 1$, the IW func-

tion has the form

$$\xi(\omega) = 1 - \rho^2(\omega - 1) + O((\omega - 1)^2), \tag{2.4}$$

where ρ^2 is the slope of the Isgur-Wise function at $\omega = 1$.

The differential decay rate for the process discussed above is given by [5]

$$\frac{d\Gamma(\bar{B} \to D^* \ell \bar{\nu})}{d\omega} = \frac{G_F^2}{48\pi^3} (m_{\bar{B}} - m_{D^*})^2 m_{D^*}^3 \eta_A^2 \sqrt{\omega^2 - 1} (\omega + 1)^2 \left[1 + \frac{4\omega}{\omega + 1} \frac{1 - 2\omega r + r^2}{(1 - r)^2}\right] |V_{cb}|^2 \xi^2(\omega), \tag{2.5}$$

where $r = \frac{m_{D^*}}{m_{\bar{B}}}$ and η_A is a constant which is present due to a finite renormalization of the axial vector current.

It is clear from the above expression that knowledge of the differential decay rate and of the Isgur-Wise function would allow us to calculate V_{cb}. However, as is evident from Eq. (2.3), we need to know the meson wave functions to calculate the Isgur-Wise function. In the next section we show how to do this using a covariant reduction of the BSE.

III. MESON WAVE FUNCTIONS FROM THE BSE

In a previous set of works, reductions of the BSE have been solved for $q\bar{q}$ systems [13, 14]. In this section we shall briefly describe our treatment and the wave functions resulting from our calculation. The actual equations solved to obtain these wave functions are given in the Appendix and the reader is referred to the previous works cited above for a full treatment.

The BSE is a covariant four-dimensional wave equation for relativistic bound states and is very challenging to solve exactly for realistic kernels. One typically uses several approximations to reduce it to a solvable form. We have used a quasipotential equation framework to reduce the BSE to the three-dimensional integral equation introduced in [13] and have retained only the ladder diagram component of the full BSE kernel. Under this approximation the interaction kernel contains a one-gluon exchange term $V_{\rm OGE}$, to which we add a phenomenological, long-range confining potential $V_{\rm con}$. The interaction kernel that we use is thus derived from the potential

$$V_{\rm OGE} + V_{\rm con} = \frac{4}{3}\alpha_s \frac{\gamma_\mu \otimes \gamma_\mu}{(q - q')^2} + \sigma \lim_{\mu \to 0} \frac{\partial^2}{\partial \mu^2} \frac{\mathbf{1} \otimes \mathbf{1}}{-(q - q')^2 + \mu^2}. \tag{3.1}$$

Here, α_s is the strong coupling, which is weighted by the meson color factor of $\frac{4}{3}$, and the string tension σ is the strength of the confining part of the interaction.

We also take into account the running of the strong coupling constant. Specifically, we use the form

$$\alpha_s(Q^2) = \frac{4\pi\alpha_s(\mu^2)}{4\pi + (11 - 2n_f/3)\alpha_s(\mu^2)\ln(Q^2/\mu^2)}, \tag{3.2}$$

where

$$Q^2 = \gamma^2 M_{\rm meson}^2 + \beta^2, \tag{3.3}$$

and where γ and β are parameters determined by a fit to the meson spectrum. n_f in Eq. (3.2) corresponds to

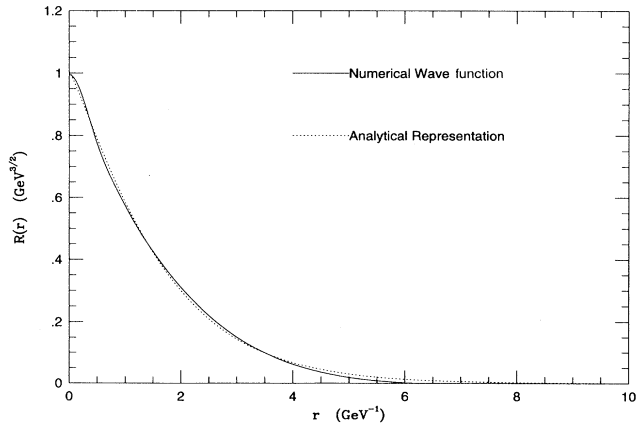

FIG. 1. Radial wave function for the $\bar{B}$ meson. The solid line represents the numerical solution of the BSE. This is obtained from the Fourier transform of $\psi^0(q)$ appearing in Eq. (A1). The entire Fourier transform of $\psi^0(q)$ in position space is normalized to unity. An analytical approximation to $\psi^0(q)$ is given in Eq. (3.4) (with $\lambda = 0.59$ GeV and $n = 1.16$) and is represented by the dashed line.

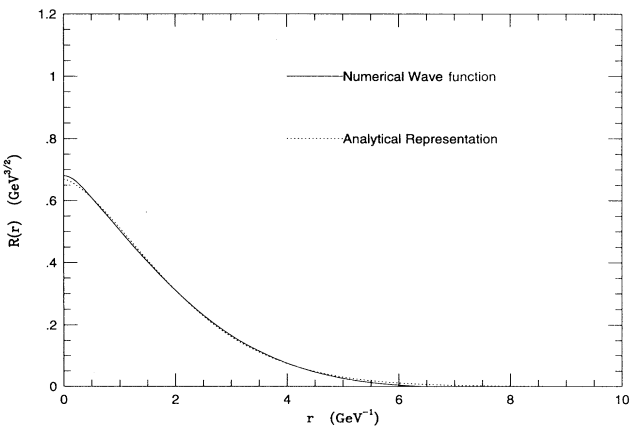

FIG. 2. Radial wave function for the D^* meson. The solid line represents the numerical solution of the $l = 0$ component. This is obtained from the Fourier transform of $\psi_0^1(q)$ appearing in Eq. (A5). The entire Fourier transform of $\psi_0^1(q)$ in position space is normalized to unity. An analytical approximation to $\psi_0^1(q)$ is given in Eq. (3.4) (with $\lambda = 0.42$ GeV and $n = 1.52$) and is represented by the dashed line.

the number of flavors which was taken to be 4 [13, 14]. In the above equation μ is taken to be the mass of the Z boson and $\alpha_s(\mu^2)$ is correspondingly chosen to be equal to 0.12 based on experimental measurements.

In our formulation of the BSE there are seven parameters: four masses m_u=m_d, m_c, m_s, m_b; the string tension σ; and the parameters γ and β used to govern the running of the coupling constant. These parameters were determined by fitting the meson masses calculated from the BSE to the observed spectrum. We utilize this BSE model for the mesons to evaluate the meson wave functions. The wave functions for B and D^* mesons are shown in Figs. 1 and 2, respectively. For the purpose of further calculations we have also obtained analytic representations of these wave functions:

$$\psi(x,y,z) = \left(\frac{(2^{1/n}\lambda)^3 n}{\Gamma(\frac{3}{n})}\right)^{1/2} e^{-\lambda^n (x^2+y^2+z^2)^{n/2}}, \quad (3.4)$$

where λ = 0.59 GeV, n = 1.16 for the $\bar{B}$ meson and λ = 0.42 GeV, n = 1.52 for the D^* meson. We have plotted the numerical wave functions and their analytic representations together to display the accuracy of the latter. For convenience, we shall use these analytical expressions for subsequent calculations in this paper.

IV. ISGUR-WISE FUNCTION AND V_{cb}

In this section we shall describe our results using the ingredients that have been presented above. Using Eq. (2.3) and taking into account the relativistic boost (assumed along the z direction), the IW function can be written as [10]

$$\xi(\omega) = \left(\frac{2}{\omega+1}\right)^{1/2} \int \psi^*_{lD^*}(x,y,\omega z)\psi_{l\bar{B}}(x,y,z)e^{iEz\sqrt{\omega^2-1}}d^3x, \quad (4.1)$$

where E is the mass of the light component of the D^* meson in the rest frame of the B meson.

We use the wave functions derived from the BSE to evaluate the IW function and we emphasize again that our IW function involves no additional parameter fitting. The plot of our IW function is shown in Fig. 3. It is interesting to note that since the wave functions used are coming from the BSE which is solved independent of the heavy quark approximation, the IW function does not go to unity at zero recoil. The deviation of the IW function from unity at zero recoil can be attributed to the finite mass effects which are incorporated in our BSE model (implicitly to all orders in 1/mass). We have also obtained an analytical representation as a best fit to the IW function that is plotted in Fig. 3. This is given by

$$\xi(\omega) = \eta\left[1 - \frac{\rho^2}{\eta}(\omega-1) + a(\omega-1)^{3/2}\right], \quad (4.2)$$

where ρ^2 = 1.279, a = 0.91, and η = 0.9942.

We can now use the IW function as calculated above to extract V_{cb} from the experimental data for $\bar{B} \to D^* \ell \bar{\nu}$ decay. We have used the data from ARGUS 93 [7], CLEO 93 [8], and CLEO 94 [9] and the corresponding fits to these data using our IW function are shown in the Figs. 4, 5, and 6, respectively.

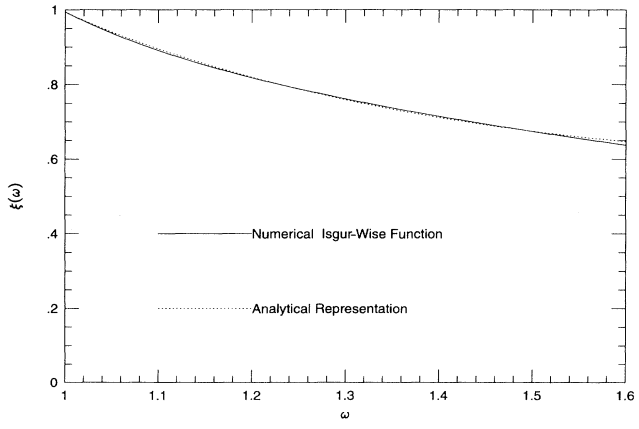

FIG. 3. The Isgur-Wise function. The solid line represents the IW function calculated from Eq. (4.1). An analytical approximation to the IW function is given in Eq. (4.2) and is represented by the dashed line. The deviation of the IW function from unity at zero recoil is due to the finite heavy quark mass effects incorporated in our BSE model.

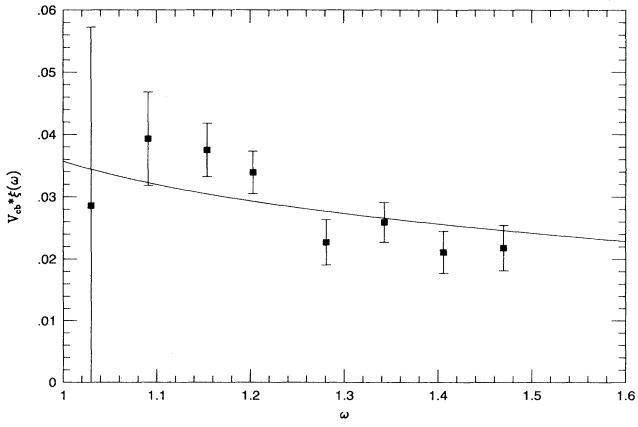

FIG. 4. Plot of $V_{cb}\,\xi(\omega)$ vs ω from ARGUS 93 data of $\bar{B} \to D^* \ell \bar{\nu}$ decay [7]. The data points for $V_{cb}\,\xi(\omega)$ are extracted from the experimental result by using Eq. (2.5). The solid line represents our best fit to the data.

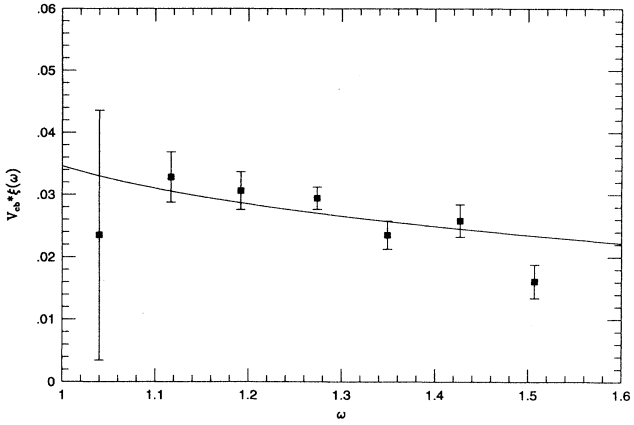

FIG. 5. Plot of $V_{cb}\,\xi(\omega)$ vs ω from CLEO 93 data of $\bar{B} \to D^*\ell\bar{\nu}$ decay [7]. The data points for $V_{cb}\,\xi(\omega)$ are extracted from the experimental result by using Eq. (2.5). The solid line represents our best fit to the data.

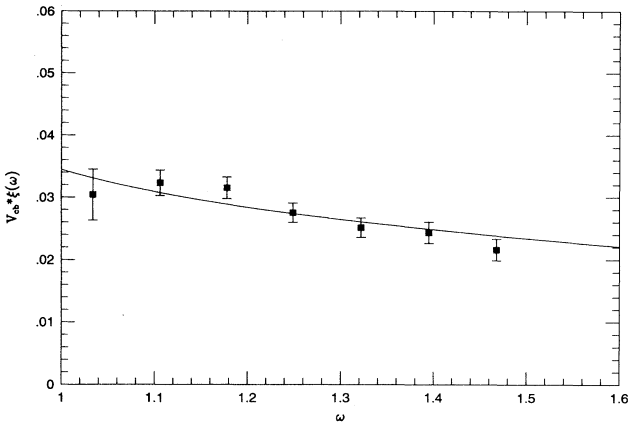

FIG. 6. Plot of $V_{cb}\,\xi(\omega)$ vs ω from CLEO 94 data of $\bar{B} \to D^*\ell\bar{\nu}$ decay [7]. The data points for $V_{cb}\,\xi(\omega)$ are extracted from the experimental result by using Eq. (2.5). The solid line represents our best fit to the data.

In Table I we present the different values of V_{cb} (in units of 10^{-3}) obtained from these experimental data [for each set of experimental data we have shown two values of V_{cb}, one obtained from the numerical calculation of the IW function and the other from its analytic representation as given in Eq. (4.2)]. The uncertainties in the values of V_{cb} tabulated above are determined by fitting to the two extreme values appearing on the experimental error bars. The different values thus obtained are consistent with each other and are comparable to some of the latest estimates of V_{cb} [4–6].

V. CONCLUSION

We have used the solutions of the BSE to predict the shape of the IW function. Such a prediction is independent of any undetermined parameter. The solution of the BSE does not depend on the heavy quark approximation and the corresponding IW function calculated from its solutions incorporates some of the finite mass corrections. This is evident from the fact that in our calculation the IW function deviates from unity at zero recoil. We have also found a simple analytical representation that best fits the numerically computed IW function. Using the IW function we have calculated V_{cb} from the latest set of experimental data. Our best estimate of $V_{cb} = (34.7 \pm 2.5) \times 10^{-3}$ is comparable to the latest estimates of V_{cb} available in the literature [4–6].

From knowledge of the solutions of the BSE it should be possible to calculate the four form factors in Eq. (2.1) directly without using the heavy quark limit. Such a calculation would provide an interesting test of the accuracy and consistency of the heavy quark approximation and is currently being pursued.

ACKNOWLEDGMENTS

We thank A.P. Balachandran, C. Benesh, M. Burkardt, M. Harada, G. Moneti, A. Petridis, J.W. Qiu, J. Schechter, S. Stone, and B.-L. Young for discussions. K.S.G. acknowledges the hospitality of the Physics Department of Syracuse University where a part of this work was completed. This work was supported in part by the U.S. Department of Energy, Grant No. DE-FG02-87ER40371, Division of High Energy and Nuclear Physics.

APPENDIX: BETHE-SALPETER EQUATIONS

In this appendix we present the BSE's that have been solved. This is done for the sake of completeness and the reader should refer to [13, 14] for further details.

The BSE for the 0^- channel is given by

$$[(E_1 + E_2)^2 - E^2]\psi^0(q) = \frac{E}{\pi q}[I_0^{\rm con}\psi^0(q') + I_0^{\rm OGE}\psi^0(q')], \tag{A1}$$

and those for the 1^- channel are given by

TABLE I. Values of V_{cb} in the units of 10^{-3} from different sets of experimental data. The first row indicates the values of V_{cb} obtained by using the IW function that was calculated numerically. The second row indicates the corresponding values of V_{cb} obtained by using an analytical approximation to the IW function as given in Eq. (4.2).

	ARGUS 93	CLEO 93	CLEO 94
From numerical IW function	(35.8 ± 8.3)	(34.8 ± 6.1)	(34.7 ± 2.5)
From analytical IW function	(35.9 ± 8.3)	(34.8 ± 6.1)	(34.7 ± 2.5)

$$[(E_1+E_2)^2-E^2]\psi^{12}(q)=\frac{E}{\pi q}[(I_1^{\rm con}+I_1^{\rm OGE})\psi^{12}(q')+(I_2^{\rm con}+I_2^{\rm OGE})\psi^{34}(q')] \tag{A2}$$

and

$$[(E_1+E_2)^2-E^2]\psi^{34}(p)=\frac{E}{\pi q}[(I_3^{\rm con}+I_3^{\rm OGE})\psi^{12}(q')+(I_4^{\rm con}+I_4^{\rm OGE})\psi^{34}(q')]. \tag{A3}$$

The symbols appearing in the above equations are defined as

$$I_0^{\rm con}=\sigma\lim_{\mu\to0}\frac{\partial^2}{\partial\mu^2}\int_0^\infty dq'q'[Q_0(z')T_0^{\rm con}+Q_0^1(z')T_1^{\rm con}],$$

$$I_1^{\rm con}=\sigma\lim_{\mu\to0}\frac{\partial^2}{\partial\mu^2}\int_0^\infty dq'q'[Q_0(z')T_1^{\rm con}+Q_0^1(z')T_2^{\rm con}],$$

$$I_2^{\rm con}=\sigma\lim_{\mu\to0}\frac{\partial^2}{\partial\mu^2}\int_0^\infty dq'q'[Q_1^3(z')T_2^{\rm con}],$$

$$I_3^{\rm con}=\sigma\lim_{\mu\to0}\frac{\partial^2}{\partial\mu^2}\int_0^\infty dq'q'[Q_1^3(z')T_2^{\rm con}],$$

$$I_4^{\rm con}=\sigma\lim_{\mu\to0}\frac{\partial^2}{\partial\mu^2}\int_0^\infty dq'q'[Q_1(z')T_1^{\rm con}+Q_1^2(z')T_0^{\rm con}],$$

$$I_0^{\rm OGE}=\frac{q\alpha_s}{3}\int_0^\infty dq'q'[Q_0(z)T_0^{\rm OGE}+Q_0^1(z)T_1^{\rm OGE}],$$

$$I_1^{\rm OGE}=\frac{q\alpha_s}{3}\int_0^\infty dq'q'[Q_1(z)T_3^{\rm OGE}+Q_1^1(z)T_4^{\rm OGE}],$$

$$I_2^{\rm OGE}=\frac{q\alpha_s}{3}\int_0^\infty dq'q'[Q_1^3(z)T_5^{\rm OGE}],$$

$$I_3^{\rm OGE}=\frac{q\alpha_s}{3}\int_0^\infty dq'q'[Q_1^3(z)T_7^{\rm OGE}],$$

$$I_4^{\rm OGE}=\frac{q\alpha_s}{3}\int_0^\infty dq'q'[Q_1(z)T_2^{\rm OGE}+Q_1^2(z)T_1^{\rm OGE}],$$

$$T_0^{\rm con}=\frac{-1}{2(E_1E_2E_1'E_2')}(E_1E_2E_1'E_2'+q^2q'^2),$$

$$T_1^{\rm con}=\frac{1}{2(E_1E_2E_1'E_2')}qq'(E_1E_1'+E_2E_2'),$$

$$T_2^{\rm con}=\frac{1}{2(E_1E_2E_1'E_2')}(E_1E_2E_1'E_2'-q^2q'^2),$$

$$T_0^{\rm OGE}=\frac{1}{4(E_1E_2E_1'E_2')}(E_1E_2E_1'E_2'+q^2q'^2+3q^2E_1'E_2'+3q'^2E_1E_2),$$

$$T_1^{\rm OGE}=\frac{1}{4(E_1E_2E_1'E_2')}(E_1E_2E_1'E_2'+q^2q'^2+q^2E_1'E_2'+q'^2E_1E_2),$$

$$T_2^{\rm OGE}=\frac{1}{4(E_1E_2E_1'E_2')}qq'(E_1E_1'+E_2E_2'+E_1'E_2+E_1E_2'),$$

$$T_3^{\rm OGE}=\frac{1}{4(E_1E_2E_1'E_2')}4qq'(E_1E_1'+E_2E_2'),$$

$$T_4^{\rm OGE}=\frac{1}{4(E_1E_2E_1'E_2')}(E_1E_2E_1'E_2'+q^2q'^2-q^2E_1'E_2'-q'^2E_1E_2),$$

$$T_5^{\rm OGE}=\frac{-1}{4(E_1E_2E_1'E_2')}(E_1E_2E_1'E_2'-q^2q'^2+q^2E_1'E_2'-q'^2E_1E_2),$$

$$T_6^{\rm OGE}=\frac{1}{4(E_1E_2E_1'E_2')}qq'(E_1-E_2)(E_1'-E_2'),$$

$$T_7^{\rm OGE}=\frac{-1}{4(E_1E_2E_1'E_2')}(E_1E_2E_1'E_2'-q^2q'^2-q^2E_1'E_2'+q'^2E_1E_2), \tag{A4}$$

where

$$E_1 = (m_1^2 + q^2)^{\frac{1}{2}}, \qquad E_2 = (m_2^2 + q^2)^{\frac{1}{2}},$$
$$E_1' = (m_1^2 + q'^2)^{\frac{1}{2}}, \qquad E_2' = (m_2^2 + q'^2)^{\frac{1}{2}},$$
$$z = \frac{q^2 + q'^2}{2qq'}, \qquad z' = \frac{q^2 + q'^2 + \mu^2}{2qq'}.$$

In the above equations, Q_j are the Legendre polynomials of the second kind and

$$Q_j^1(z) = zQ_j(z) - \delta_{j0},$$
$$Q_j^2(z) = \frac{1}{j+1}[jzQ_j(z) + Q_{j-1}(z)],$$
$$Q_j^3(z) = \left(\frac{j}{j+1}\right)^{\frac{1}{2}}[zQ_j(z) + Q_{j-1}(z)].$$

Finally, we also have

$$\psi^j_{l=j-1}(q) = \frac{i(-j+1)}{[2(2j+1)]^{\frac{1}{2}}}[j^{\frac{1}{2}}\psi^{12\ j}(q) + (j+1)^{\frac{1}{2}}\psi^{34\ j}(q)],$$
$$\psi^j_{l=j+1}(q) = \frac{i(-j-1)}{[2(2j+1)]^{\frac{1}{2}}}[-(j+1)^{\frac{1}{2}}\psi^{12\ j}(q) + j^{\frac{1}{2}}\psi^{34\ j}(q)]. \tag{A5}$$

$\psi^{12\ j}(q)$ and $\psi^{34\ j}(q)$ are obtained by numerically solving Eqs. (A2) and (A3). $\psi^j_{l=j-1}(q)$ and $\psi^j_{l=j+1}(q)$ are then obtained numerically from Eq. (A5). These are the wave functions for the D^* meson. The $l = 2$ component of the D^* meson wave function is negligible in comparison to the $l = 0$ component and is neglected. Similarly, $\psi^0(q)$ (representing the wave function of the $\bar{B}$ meson) is obtained by numerically solving Eq. (A1). Analytical approximations of $\psi^0(q)$ and $\psi^1_1(q)$ are given in Eq. (3.4). They are used in Eq. (4.1) to calculate the IW function. Figures 1 and 2 show the numerical wave functions and their analytical representations for $\bar{B}$ and D^* mesons, respectively.

[1] N. Isgur and M. B. Wise, Phys. Lett. B **232**, 113 (1989); **237**, 527 (1990).
[2] M. B. Voloshin and M. A. Shifman, Yad. Fiz. **47**, 801 (1988) [Sov. J. Nucl. Phys. **47**, 511 (1988)].
[3] H. Georgi, Phys. Lett. B **240**, 447 (1990).
[4] M. Neubert, Phys. Rep. **245**, 259 (1994), and references therein.
[5] M. Neubert, Phys. Lett. B **338**, 84 (1994).
[6] S. Stone, Syracuse University Report No. HEPSY 94-5, 1994 (unpublished).
[7] ARGUS Collaboration, A. Albrecht *et al.*, Z. Phys. C **57**, 533 (1993).
[8] CLEO Collaboration, G. Crawford *et al.*, in *Lepton and Photon Interactions*, Proceedings of 16th International Symposium, Ithaca, New York, 1993, edited by P. Drell and D. Rubin, AIP Conf. Proc. No. 302 (AIP, New York, 1994).
[9] CLEO Collaboration, B. Barish *et al.*, Phys. Rev. D **51**, 1014 (1995).
[10] M. Neubert and V. Rieckert, Nucl. Phys. **B382**, 97 (1992).
[11] E. E. Salpeter and H. A. Bethe, Phys. Rev. **84**, 1232 (1951).
[12] T. Kugo, M. G. Mitchard, and Y. Yoshida, Prog. Theor. Phys. **91**, 521 (1994).
[13] A. J. Sommerer, J. R. Spence, and J. P. Vary, Phys. Rev. C **49**, 513 (1994).
[14] A. J. Sommerer, A. Abd El-Hady, J. Spence, and J. P. Vary, Iowa State University Report No. ISU-NP-94-07, 1994 (unpublished).